7-2014

Studies of a mathematical model for generating rhythmic behavior with a simple brain

Juan C. Morales
University of Texas-Pan American

STUDIES OF A MATHEMATICAL MODEL FOR GENERATING RHYTHMIC BEHAVIOR WITH A SIMPLE BRAIN

A Thesis

by

JUAN C. MORALES

Submitted to the Graduate School of
The University of Texas-Pan American
In partial fulfillment of the requirements for the degree of

MASTER OF SCIENCE

July 2014

Major Subject: Applied Mathematics

STUDIES OF A MATHEMATICAL MODEL FOR GENERATING RHYTHMIC BEHAVIOR WITH A SIMPLE BRAIN

A Thesis
by
JUAN C. MORALES

COMMITTEE MEMBERS

Dr. Virgil Pierce
Chair of Committee

Dr. Daniel Plas
Co-Chair of Committee

Dr. Maria Cristina Villalobos
Committee Member

Dr. Eleftherios Gkioulekas
Committee Member

July 2014

ABSTRACT

Morales, Juan C., Studies of a Mathematical Model for Generating Rhythmic Behavior with a Simple Brain . Master of Science (MS), July, 2014, 28 pages, 3 tables, 16 figures, 6 references.

The rhythmic behavior of feeding in the pond snail, *Lymnaea stagnalis* can be described computationally by a model describing its central pattern generator network (CPG). The model includes coupled Hodgkin-Huxley type nonlinear ordinary differential equations describing four neurons connected by both inhibitory and excitatory synapses. We studied the system's dependence on current parameters to generate periodic behavior. We also considered the effect of eliminating specific connections from the network. In addition, experiments on the biological system were used to motivate application of the model in Parkinson's disease.

DEDICATION

I would like to dedicate this manuscript to my mother, grandmother, sisters, nieces, and the rest of my family and friends.

ACKNOWLEDGMENTS

I would like to thank all of the people that helped me prepare this manuscript. I would specifically like to thank:

- The **GAANN** team. GAANN allowed me to prioritize my education.
- Dr. **Virgil Pierce** who allowed the freedom to search for an interesting project. Not only was Dr. Pierce of great assistance with the mathematics of the project, but he also offered great advice which allowed me to make great educational decisions.
- Dr. **Daniel Plas** who allowed me to join his lab. This allowed me to gain invaluable experience. He has provided a substantial amount of help with the biology component of the project. Dr. Plas also provided invaluable advice and preparation for the next step of my academic career.
- Dr. **Cristina Villalobos** who has been a great mentor dating back to my time as an undergraduate. She is an inspiring figure who is always willing to guide and advice those pursuing a higher education.
- Dr. **Eleftherios Gkioulekas** for agreeing to be a part of my committee despite such short notice.

Lastly, I would like to thank **UTPA** for the educational opportunity.

TABLE OF CONTENTS

LIST OF TABLES

Page

LIST OF FIGURES

Page

CHAPTER I

INTRODUCTION

The most important topic in neurobiology is to understand how the underlying biology and neural circuitry ultimately lead to the final output: behavior. Understanding complex human behavior is a formidable task as it involves complex interactions between billions of cells.

1.1 The Nervous System and the Neuron

Cells in the nervous systems vary in morphology, and possess electrical properties that allow for communication within a *neuron*. Stereotypical neurons contain three compartments that participate in the process of communication: *(a) Dendrites*; *(b) Cell Body (Soma)*; *(c) Axon*.

Loosely speaking, *dendrites* receive input, the *soma* integrates the input, and the result travels down the *axon* as the final output. This result takes the form of a transient change in voltage across the membrane that is called the action potential. Additionally, this output is transmitted to a follower neuron by release of a neurotransmitter substance at a synapse. Although there may be many dendrites in a neuron, there is only one soma and one axon. These two compartments may vary in length and size. From a combinatorial point of view, there are many different versions of the neuron.

1.2 Central Pattern Generators and Rhythmic Behavior

A single neuron is of no use if it cannot communicate with other neurons. Understanding the communication process can be complex, as even simple behaviors like chewing require interactions between many neurons. Chewing is just one example of rhythmic behaviors that are found throughout the animal kingdom. It has been found that these behaviors are produced by dedicated

networks called *central pattern generators* (CPG). Other well known CPGs govern behaviors such as breathing, walking, and swimming.

The CPGs that have been studied share common features including a small network of neurons, mutual excitation and inhibition, phase locking, and the occurence of bursting neurons. In addition to providing insight into these specific behaviors, the study of central pattern generators gives us a tool to study neuronal communication in general.

1.3 Feeding in *Lymnaea stagnalis*

Lymnaea stagnalis is a freshwater gastropod that is found in Northern United States, Europe, and Asia. It is approximately three centimeters in length and primarily feeds on plants.

Feeding in the pond snail is rhythmic and exhibits a stereotyped sequence. First, in *protraction* the snail protrudes a tongue like structure called the radula. Next, in *retraction* the radula scrapes the food surface as it is drawn back into the mouth. Finally, in the *swallow* phase the food enters the esophagus.

This basic cycle can be produced using a minimum of three neurons in the appropriate configuration. These neurons have been given the names N1 Medial *(N1M)*, N2 ventral *(N2v)*, and N3 tonic *(N3t)*. The number (1,2, or 3) in each neuron's name indicates the phase during which that neuron fires. Thus, N1M fires during protraction, N2v during retraction, and N3t during the swallow phase. These neurons are found in close proximity within a paired set of structures called the buccal ganglia. The basic feeding cycle can be modulated by extrinsic neurons. An important modulatory neuron found in the buccal ganglion is called the slow oscillator *(SO)*.

1.4 Hodgkin - Huxley Model

The well known Hodgkin-Huxley (HH) equations have been extensively used as a model for the action potential [2]. These equations were developed using electrophysiological data recorded from the giant axon of the squid and have been found to apply to neurons generally. The HH equations model the membrane as an electronic device in which capacitance and time varying resistances act in parallel. The model becomes more elaborate as more cell features are incorporated.

The HH equations are of the form:

$$C_m \frac{dV}{dt} = I - \bar{g}_L(V - E_L) - \bar{g}_{Na} p^3 h(V - E_{Na}) - \bar{g}_K q^4 (V - E_K) \tag{1.1}$$

$$\frac{dp}{dt} = \frac{p_\infty(V) - p}{\tau_p(V)}, \tag{1.2}$$

$$\frac{dq}{dt} = \frac{q_\infty(V) - q}{\tau_q(V)}, \tag{1.3}$$

$$\frac{dh}{dt} = \frac{h_\infty(V) - h}{\tau_h(V)}, \tag{1.4}$$

where C_m is the membrane capacitance measured in μF, $\bar{g}$ is the maximal conductance measured in μS, and p, q, and h are dimensionless 'gating' variables. The gating variables are time dependant and describe the dynamics of the open and closed states of specific ion channels in the membrane. The gating variables are probabilities (p,q,$h \in$ [0,1]). The exponent in each gating variable represents the number of activation and inactivation gates.The asymptotic values, p_∞, q_∞, h_∞ are of the form:

$$g_\infty(V) = \frac{\alpha_g(V)}{\alpha_g(V) + \beta_g(V)}, \tag{1.5}$$

where $g \in \{p, q, h\}$. Moreover, $\alpha_g(V)$, and $\beta_g(V)$ involve V exponentially. These terms vary by ionic species. They resemble Gaussian or sigmoid curves. Finally, the value E_x, represents the equilibrium potential with respect to a specific ionic species, x, where x represents either sodium (Na) or potassium (K). The equilibrium potential is found using the standard *Nernst Equation*,

$$E_x = \frac{RT}{zF} ln(\frac{[out]_x}{[in]_x}). \tag{1.6}$$

In equation (1.6), R is Boltzmann's gas constant, T is absolute temperature, F is Faraday's constant, and z is the charge of the respective ion. The term $[out]_x$ represents the concentration of the ion x outside the cell while $[in]_x$ represents the concentration inside.

As written, equation (1.1) is in units of current (nA).If the equation is multiplied by the

membrane resistance, R_m, measured in $M\Omega$, the result expresses units of millivolts:

$$R_m C_m \frac{dV}{dt} = R_m(I - \bar{g}_L(V - E_L) - \bar{g}_{Na} p^3 h(V - E_{Na}) - \bar{g}_K q^4 (V - E_K)), \tag{1.7}$$

$$\frac{dp}{dt} = \frac{p_\infty(V) - p}{\tau_p(V)}, \tag{1.8}$$

$$\frac{dq}{dt} = \frac{q_\infty(V) - q}{\tau_q(V)}, \tag{1.9}$$

$$\frac{dh}{dt} = \frac{h_\infty(V) - h}{\tau_h(V)}. \tag{1.10}$$

Now, let $R_m C_m = \tau_m$ be the membrane time constant measured in milliseconds. Because $R_m = \frac{1}{\bar{g}_L}$, multiplication leads to cancellation of conductance units. The result is a dimensionless scalar, γ, with $\gamma \in \mathbb{R}$. Thus by Ohm's law, we now have a voltage measured in millivolts. This algebraic manipulation leads to the equations,

$$\tau_m \frac{dV}{dt} = IR_m - (V - E_L) - \gamma_{Na} p^3 h(V - E_{Na}) - \gamma_K q^4 (V - E_K), \tag{1.11}$$

$$\frac{dp}{dt} = \frac{p_\infty(V) - p}{\tau_p(V)}, \tag{1.12}$$

$$\frac{dq}{dt} = \frac{q_\infty(V) - q}{\tau_q(V)}, \tag{1.13}$$

$$\frac{dh}{dt} = \frac{h_\infty(V) - h}{\tau_h(V)}. \tag{1.14}$$

Units of millivolts will be used for the rest of this manuscript.

Note that the 4 variables in the HH model of a single axon, lead to dynamics that act in a subspace of $\mathbb{R}^4$. The biological inspiration of the model suggest bounded domains for voltage.

CHAPTER II

THE MODEL AND ITS PROPERTIES

The model will be described in a systematic way. I will start by showing how each neuron is modeled by a system of differential equations, continue with a description of the CPG, and finish with an exploration of a few properties of the model.

2.1 Modeling Feeding Neurons in Lymnaea

As previously stated, a neuron is made up of three compartments. Hodgkin and Huxley developed a model for neural activity in the axonal compartment of the giant squid. To argue for a more realistic model that accounts for potential in more than just the axon, *Vavoulis et al.* proposed a two compartment model of feeding neurons [4]. Fig. (2.1) describes the current terms that will change membrane potential.

The CPG can be visualized graphically by nodes and edges (Fig. 2.2). Each node represents a neuron that is being modeled by a system of differential equations. An edge represents a synapse. Moreover, circles represent inhibitory synapses while bars represent excitatory ones. As mentioned before the interplay of excitatory and inhibitory connections is commonly present in CPG networks. This network topology is known to be biologically correct based on previous experimental work [4].

There are several additions that need to be made to the basic HH equations to model feeding in *Lymnaea*. These additions must account for synaptic communication, compartment coupling and ionic terms based on *Lymnaea's* cellular properties. For example, in this particular model, synapses are modeled by alpha functions [6].

The general governing differential equation for the somatic compartment is of the form,

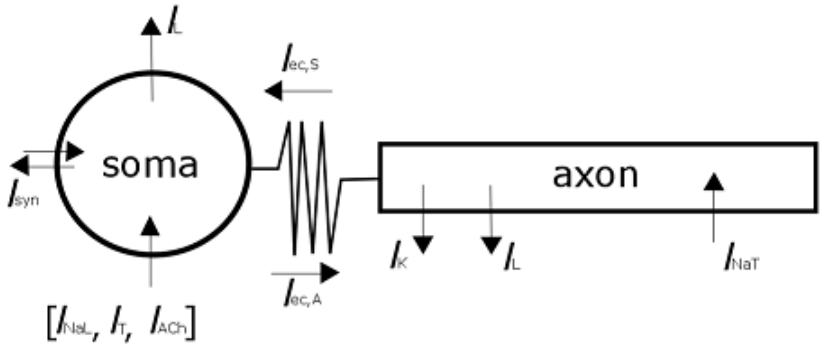

Figure 2.1: Soma coupled with Axon. Arrows directed into the compartment represent inward currents and those directed out of the compartment represent outward currents. Currents affecting the soma: I_L is the leak current, I_{syn} is the synaptic current, I_{NaL} and I_T are currents responsible for slow developing changes in the membrane potential, I_{ACh} is the current due to acetylcholine, and $I_{ec,S}$ is the current due to compartment coupling with some resistivity. Currents affecting the axon: I_K is the potassium current, I_L is the leak current, I_{NaT} is the transient sodium current and $I_{ec,A}$ is the current due to the compartment coupling with some resistivity.

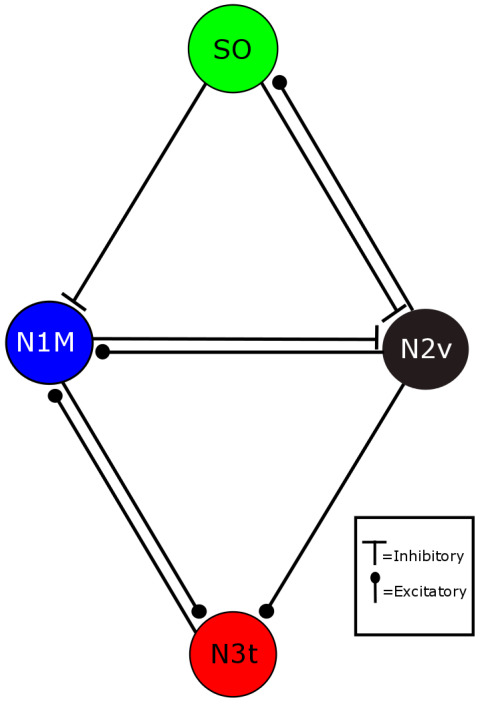

Figure 2.2: CPG of feeding in *Lymnaea stagnalis*. The 4 neurons in the basic feeding network are represented by circles (nodes). Edges represent synapses. More specifically, bars represent an inhibitory synapse while circles represent excitatory ones.

$$\tau_m \frac{dv_{i,s}}{dt} = I_{i,stim} - I_{leak,s} - I_{ion} - I_{synapse} - I_{ec,s}, \tag{2.1}$$

where $i \in \{1,2,3,4\}$. The first term in the right hand side of the equation is the stimulus term. This can be thought of as the 'forcing' term,

$$I_{i,stim} = I_{i,s}R. \tag{2.2}$$

In this particular model, R = 1.00 $M\Omega$, everywhere. The leak term encompasses a lot of information and is used for simplicity. It is of the form,

$$I_{leak,s} = v_{i,s} - E_{leak,s}, \tag{2.3}$$

where the difference, $v_{i,s}$ - $E_{leak,s}$, will be called the driving force. In general, every term other than the stimulus term and the coupling term involve a driving force. The most important term in the equation is the term that accounts for the potential changes caused by dynamical interactions between open and closed states of ion channels. It is of the form,

$$I_{ion} = \gamma_{ion}(p_i)^k_{ion}(q_i)^l_{ion}(v_{i,s} - E_{ion}), \tag{2.4}$$

where k,$l \in \{0,1,2,3,4\}$ and $ion \in \{ACh, NaL, T\}$ in this particular model. In practice exponents and ionic terms are chosen based on experimental work. Synaptic communication alter membrane potential. The term responsible for this change is,

$$I_{syn} = \sum_j \gamma_j s_j (v_{i,s} - E_{syn,j}). \tag{2.5}$$

The nonlinearity of the system is a direct consequence of the ionic and synaptic terms.
The last term accounts for the coupling between the soma and axon, and is of the form,

$$I_{ec,s} = \gamma_{ec,s}(v_{i,s} - v_{i,a}). \tag{2.6}$$

This allows the system to act as one neuron.

Similarly, the governing differential equation for the axon's potential is of the form,

$$\tau_m \frac{dv_{i,a}}{dt} = -I_{ion} - I_{ec,a} - I_{leak,a}. \tag{2.7}$$

Notice that the axonal compartment does not have a stimulus term, nor does it have a synaptic term. This occurs because the synapses occur from soma to soma. The equations for the leak and the coupling terms are defined very similarly and given by,

$$I_{leak,a} = v_{i,a} - E_{leak,a}, \tag{2.8}$$

$$I_{ec,a} = \gamma_{ec,a}(v_{i,a} - v_{i,s}). \tag{2.9}$$

The ionic term is of the form,

$$I_{ion} = \gamma_{ion}(h_i)^k_{ion}(n_i)^l_{ion}(v_{i,s} - E_{ion}), \tag{2.10}$$

where $ion \in \{NaT, K\}$ and $k, l \in \{1, 3, 4\}$.

It is important to know that intracellular and patch clamp electrophysiology in *Lymnaea*, records neural activity from the soma. Thus, solutions to the four differential equations governing the somatic compartment will replicate qualitative features seen in physiology recordings.

Differential equations governing the gating variables take on the form,

$$\frac{du_i}{dt} = \frac{u_\infty - u_i}{\tau_{u,i}}, \tag{2.11}$$

where $u \in \{p, q, h, n\}$ and $u \in [0, 1]$.

These final two equations govern the *alpha functions*, $r_j(t)$ and $s_j(t)$. These variables, r and s model synaptic transmission [6],

$$\frac{dr_j}{dt} = \frac{r_{\infty,j} - r_j}{\tau_{syn,j}}, \tag{2.12}$$

$$\frac{ds_j}{dt} = \frac{r_j - s_j}{\tau_{syn,j}}, \tag{2.13}$$

with,

$$r_{\infty,j} = \frac{1}{1 + e^{\frac{(-40 - v_{pre,i})}{2.5}}}. \tag{2.14}$$

Here $v_{pre,i}$ is the presynaptic neuron which is sending a signal to the postsynaptic cell.

Above I have given a detailed explanation of each term in the differential equations. The entire system is coupled and thus we can describe it as,

$$\tau_m \frac{d\vec{V}}{dt} = \vec{F}(\vec{V}), \tag{2.15}$$

where $\vec{V} \in \mathbb{R}^{37}$ and $\vec{F} = (f_1, f_2, ..., f_{37})$. Each f_w is smooth and more specifically each f_w is a C^1 map, for any $w \in \{1, 2, ..., 37\}$. Conductance and other parameter values were taken from previous work [4]. The tables (2.1, 2.2, 2.3) below summarize all parameter values.

Table 2.1: Parameter Values for Somatic Compartment without Synaptic Parameters

Neuron	$\bar{\gamma}_{ion}$	E_{ion} (mV)	Steady States	Time Constants $\tau_{u,i}$ (ms)
N1M	$\bar{\gamma_{ACh}} = 200$	E_{ACh} = -30	$p_{\infty,1} = (1+e^{\frac{-38.8-v_{1,s}}{10}})^{-1}$	$\tau_{p,1} = 250$
N2v	$\bar{\gamma_{NaL}} = 2$	$E_{NaL} = 55$	$p_{\infty,2} = (1+e^{\frac{-51-v_{2,s}}{10.3}})^{-1}$ $q_{\infty,2} = (1+e^{\frac{-45-v_{2,s}}{-3}})^{-1}$	$\tau_{p,2} = 28.3+44.1e^{-(\frac{-11.8-v_{2,a}}{26.6})^2}$ $\tau_{q,2} = 187.6+637.7e^{-(\frac{-9.5-v_{2,a}}{23.3})^2}$
N3t	$\bar{\gamma_T} = 3.27$	$E_T = 80$	$p_{\infty,3} = (1+e^{\frac{-61.6-v_{3,s}}{5.6}})^{-1}$ $q_{\infty,3} = (1+e^{\frac{-73.2-v_{3,s}}{-5.1}})^{-1}$	$\tau_{p,3} = 4$ $\tau_{q,3} = 400$
SO	N/A	N/A	N/A	N/A

Table 2.2: Parameter Values for Synaptic Transmission

Postsynaptic	Presynaptic	Polarity	$E_{syn,j}(mV)$	$\bar{\gamma_{syn,j}}$	$(\tau_{syn,j})$
N1M	SO	Excitatory	0	4	200
	N2v	Inhibitory	-90	50	50
	N3t	Inhibitory	-90	8	50
N2v	SO	Excitatory	0	1.0	200
	N1M	Excitatory	0	0.077	200
N3t	N1M	Inhibitory	-90	0.5	50
	N2v	Inhibitory	-90	2	50
SO	N2v	Inhibitory	-90	8	50

Table 2.3: Parameter Values for Axonal Compartment

Neuron	$\bar{\gamma_{ion}}$	$E_{ion}(mV)$	Steady States	Time Constants ($\tau_{u,i}$)
All 4 Neurons	$\bar{\gamma_{NaT}} = 350$ $\bar{\gamma_K} = 90$	$E_{NaT} = 55$ E_K = -90	$m_{\infty,i} = (1+e^{\frac{-34.6-v_{i,a}}{9.6}})^{-1}$ $h_{\infty,i} = (1+e^{\frac{-55.2-v_{i,a}}{-7.1}})^{-1}$ $n_{\infty,i} = (1+e^{\frac{-30-v_{i,a}}{17.4}})^{-1}$	$\tau_{h,i} = 1.1+7.2e^{-(\frac{-61.3-v_{i,a}}{22.7})^2}$ $\tau_{n,i} = 1.1+4.6e^{-(\frac{-61-v_{i,a}}{54.3})^2}$

Now that we have a description of the nonlinear system and the governing differential equations, we can start asking questions about the solution to the system with respect to a given initial condition.

2.2 Numerical Solution of the Nonlinear System

Modeling real phenomena can be a great task as complex behavior involves many factors. One of the complexities arises with the nonlinear nature of the problem. Nonlinearity brings difficulties in finding analytic solutions for the system. In this study we use a custom code, written in Matlab, to implement the classical fourth order Runge-Kutta method (RK4). We used a step size of one tenth of a millisecond. That is, $h = 0.1$ *ms*, and the error is of order $\mathcal{O}(h^4)$.

After using RK4 we decided to further justify qualitative features of the solution. We justified the systems insensitivity to the solver by using the built in Matlab function, *ODE45*. This built in function uses a combination of a fourth - fifth order Runge-Kutta method. An absolute error tolerance of 10^{-6} was used. Using an adaptive step size, this algorithm is able to control the error based on the chosen error tolerance. In both cases, similar qualitative features persist (Fig. 2.3, and Fig. 2.4).

2.3 Key Parameters and Properties of the Model

One of the key parameters in the system is the constant input current ($I_{i,s}$). These are present in the four differential equations governing the membrane potential of somatic compartments. This can be thought of as a 'forcing' term. We will notice that this parameter is critical for the system to enter a periodic behavior that models the three cycles seen in *Lymnaea's* feeding behavior.

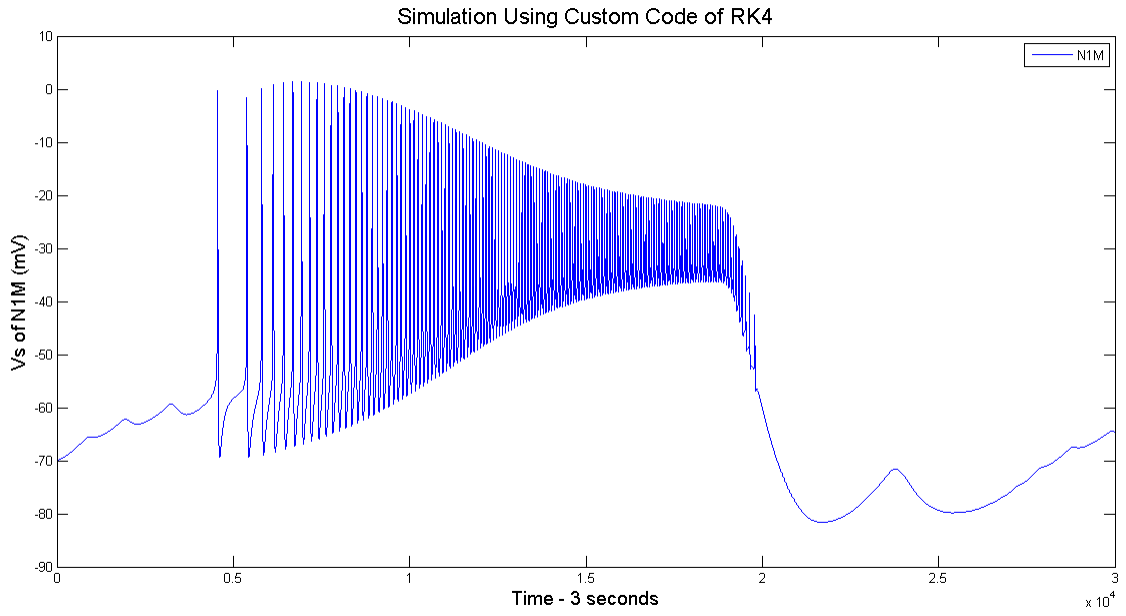

Figure 2.3: Simulation using custom code of RK4. The vertical axis denotes N1M's voltage measured in millivolts. The horizontal axis denotes the number of time steps for a total of 3 seconds.

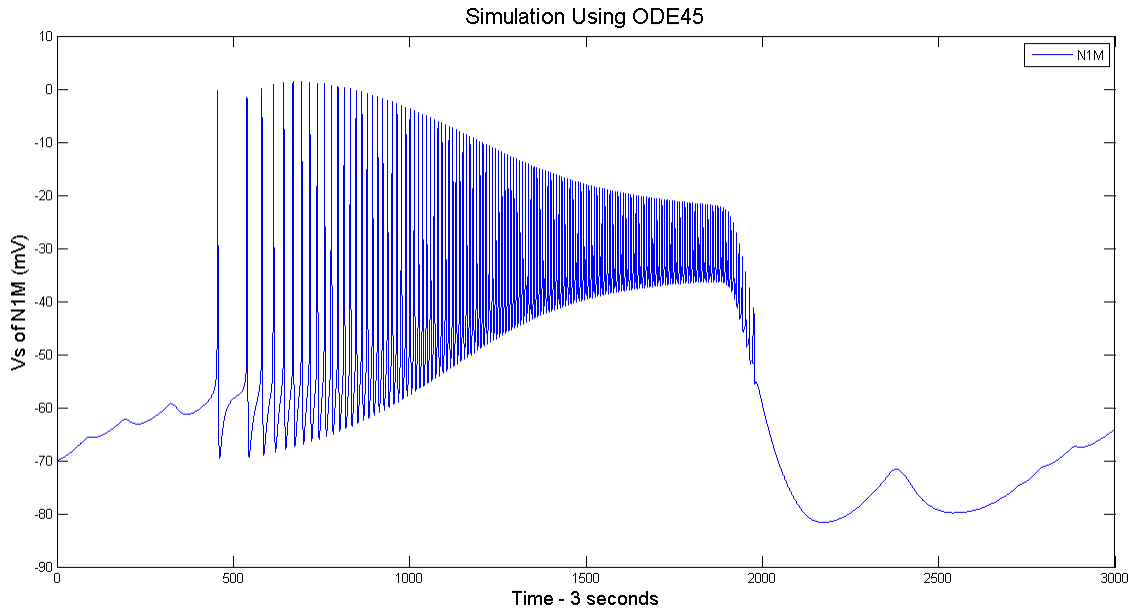

Figure 2.4: Simulation using ODE45. The vertical axis denotes N1M's voltage measured in millivolts. The horizonal axis denotes time in milliseconds for a total of 3 seconds.

Although we can think of this parameter intuitively as a 'forcing' parameter, biologically, it seems that this parameter hides many sins. It encompasses for a great deal of biochemical events occurring in the system.

For example, in preparations of the snail, it makes perfect sense for this parameter to be the injected current applied via the amplifier. This essentially forces a depolarization of the membrane and will ultimately lead to many action potentials. The perplexing aspect of this term is the fact that feeding occurs *in vivo* and thus occurs without a forcing term within the biological organism. From a biological point of view, we would like to unravel the mystery behind these parameters and be able to explain the biochemical events that make up this term. We assume that this term encompasses information coming from other parts of the snail's nervous system.

2.3.1 Current Parameters

We considered a couple of cases of the input currents importance to the system. Current parameters are important for periodic behavior.

Case 1: $I_i = 0.00\ nA$ where $i \in \{1,2,3,4\}$. In this case, application of zero current to all neurons yields tonic spiking of N3t and no triphasic behavior (Fig. 2.5). If N3t fires tonically, the result is a suppression of rasp behavior. This occurs because N3t acts as a decision making neuron. This decision is made based on the presence of food [4]. Moreover, we visualize synaptic effects by Fig. 2.6.

Case 2: $I_4 = 10.00\ nA$ and $I_i = 0.00\ nA$ where $i \in \{1,2,3\}$. Here we fed a constant current of 10.00 *nA* to SO only. All other currents were fixed at zero throughout the simulation. This leads to a rasp which lasts approximately 3 seconds (Fig. 2.7). Contrary to the first case, N3t does not fire tonically. As a consequence of N3t not firing tonically, a feeding rasp occurs and subsequent rasps continue periodically.

2.3.2 Degrading the Network

We also wanted to study what occurred if we degraded the network. We specifically investigated the case when SO was removed from the network (Fig. 2.9).

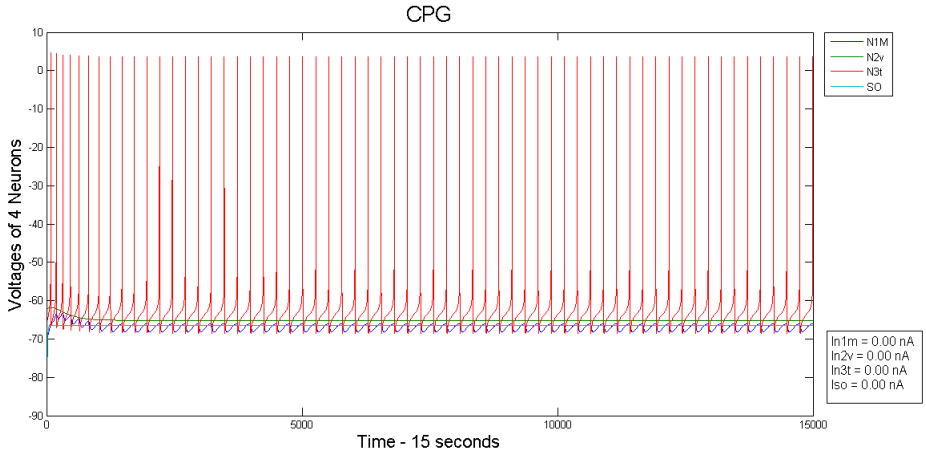

Figure 2.5: Case 1. The vertical axis is voltage measured in millivolts. The horizontal axis is time measured in milliseconds. The total time was 15 seconds. Blue is N1M, black is N2v, red is N3t and green is SO. There is no stimulus being applied to any cell.

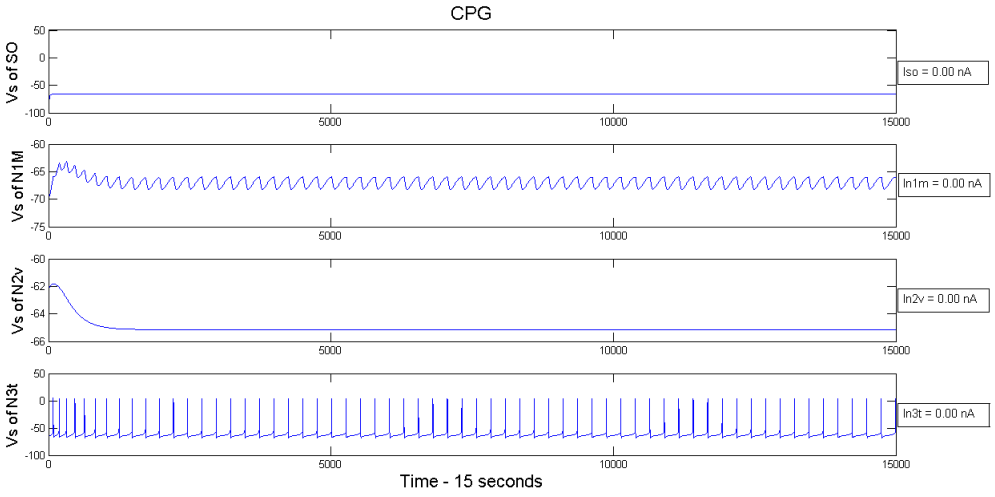

Figure 2.6: Case 1. The vertical axis is voltage measured in millivolts. The horizontal axis is time in milliseconds. This figure is a result of the same simulation ran for Fig. 2.5.

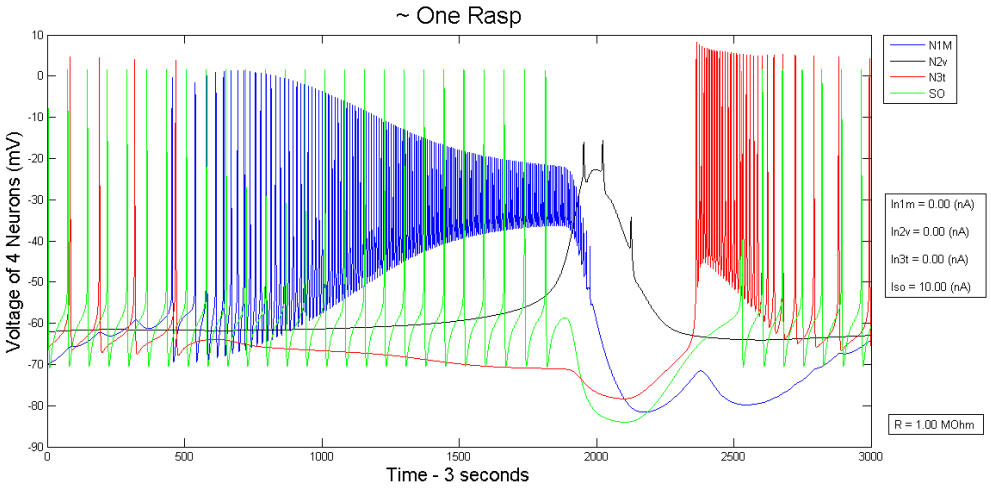

Figure 2.7: One Rasp. Constant current of 10.00 *nA* applied to SO only, enables rasping behavior. The vertical axis is voltage measured in millivolts. The horizontal axis is time measured in milliseconds.

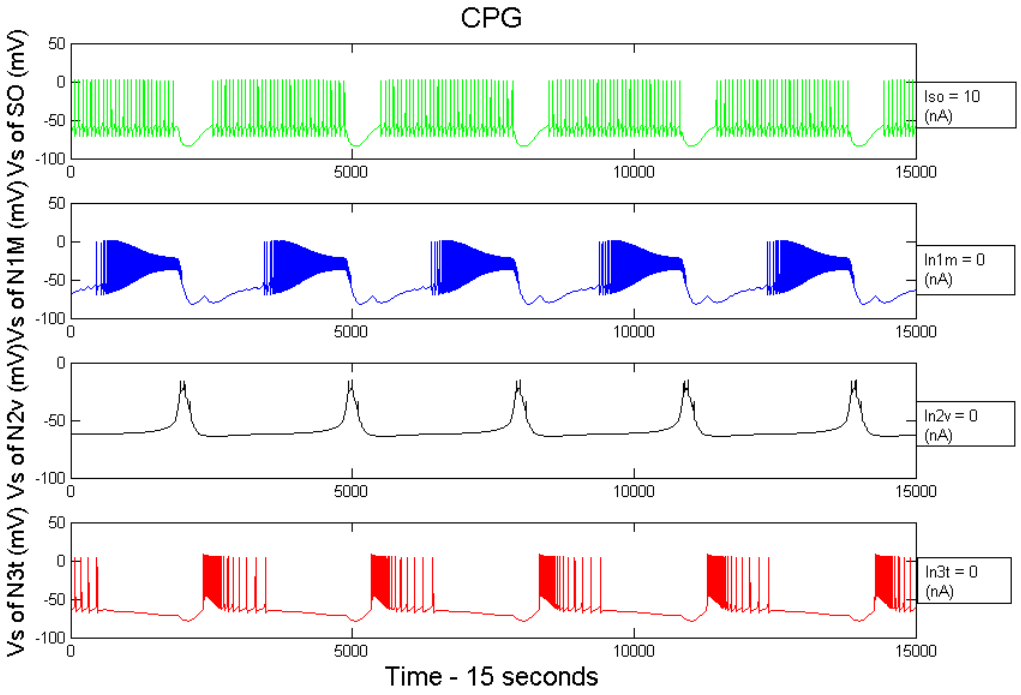

Figure 2.8: This image was generated using the simulation that produced Fig. (2.7). Again, in all four graphs, the vertical axis is voltage measured in millivolts and the horizontal axis is time. The total time was 15 seconds. Phases are clearly visible and solutions possess periodic behavior.

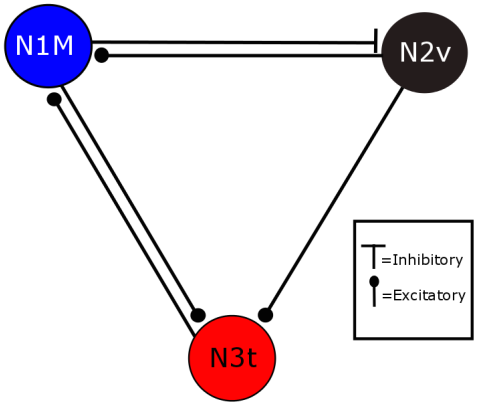

Figure 2.9: The network without SO. Removal of SO, reduces the system from 37 differential equations to 27 differential equations. Again, bars represent excitatory synapses while circles represent inhibitory synapses.

Mathematically, the nonlinear system went from having 37 differential equations to 27 differential equations. With appropriate applied current, the system was able to generate a rasp (Fig. 2.10). Moreover, with the same parameters, the system enters periodic fictive feeding (Fig. 2.11).

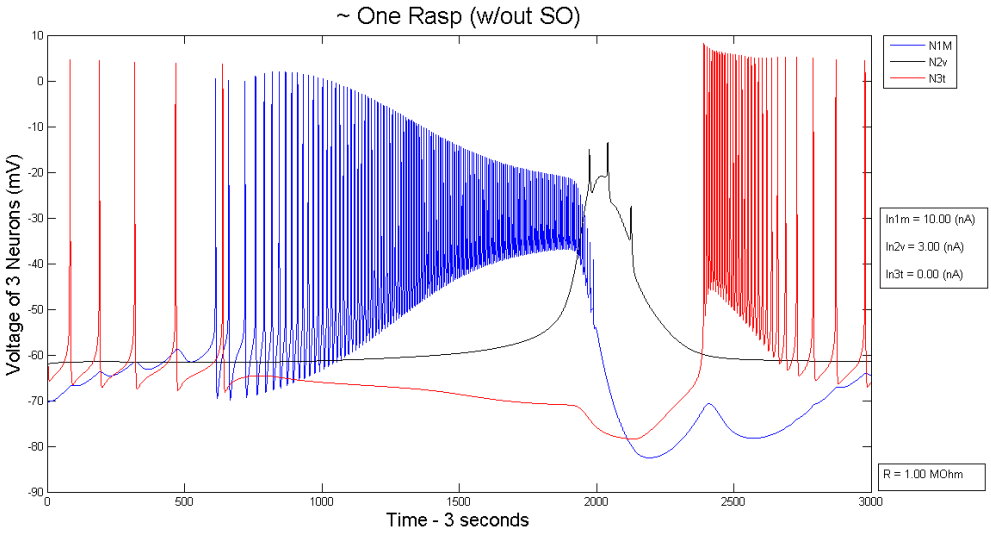

Figure 2.10: One rasp with SO removed from the network. We applied constant current of 10 *nA* to N1m. In addition simultaneously apply constant current of 3 *nA*. This allowed the system to generate a rasp and enter periodic behavior. The vertical axis is voltage measured in millivolts and on the horizontal axis we have a total time of 3 seconds. Blue represents N1M, black N2v, and red N3t.

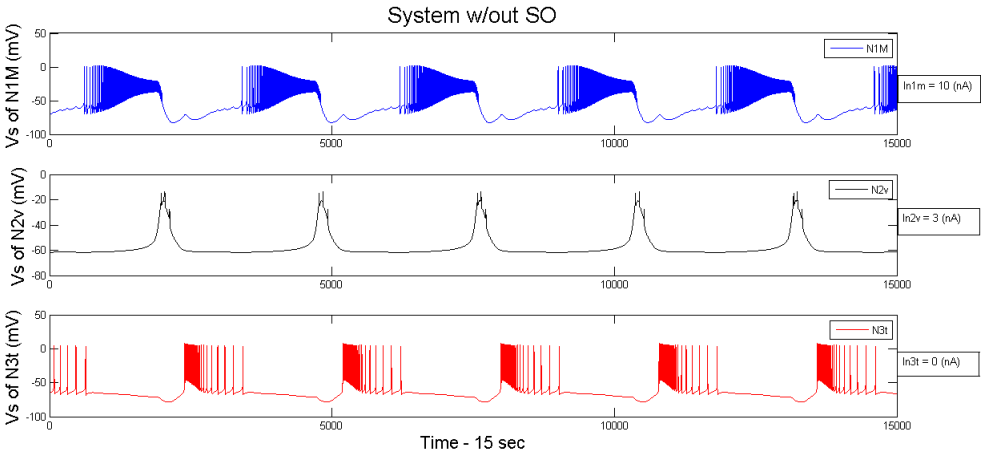

Figure 2.11: Periodic behavior with SO removed from the network. Again, we applied 10 *nA* of constant current to N1M and 3 *nA* to N2v. Each neuron and their corresponding phase is visible.

CHAPTER III

APPLICATION

3.1 Parkinson's Disease and Rotenone

Parkinson's Disease (PD) is a neurological disorder that affects over one million people in North America alone [3]. It is characterized by involuntary motor tremors and bradykinesia. Loss of dopaminergic neurons in an area of the brain known as the *substantia nigra compacta* ultimately leads to PD. Despite intensive investigation, the cause is not well understood.

The toxin, Rotenone, is known to damage dopamine cells in a variety of organisms. *Vehovsky et al.* have proposed the use of Rotenone in *Lymnaea stagnalis* as a model for studying PD [5]. It would be useful to correlate the loss of dopamine with the deficit in motor behavior. Because the CPG does not contain any dopaminergic neurons, finding this correlation is not so obvious. On the other hand, there is a small number of dopamine neurons found in the buccal ganglia. We believe that damage to one of these dopaminergic neurons may extrinsically modulate the network.

3.2 Experiment

We sought to investigate Rotenone's effect on feeding behavior in the snail. Our initial assumption was simply that that Rotenone would change the duration of the rasp. We then conducted simple feeding experiments on both control and treated groups.

3.2.1 Treatment

The snails underwent an acute rotenone treatment. An acute treatment consists of a 48 hour exposure of the snails *in vivo*. We kept the treated group in 1 liter containers that were filled with 650 mL of 0.05 μM rotenone solution. The control group was kept in 1 liter containers that were

filled with 650 mL of pond snail water.

3.2.2 Behavioral Tests

Tests were done immediately after an acute treatment. Snails were placed in a transparent rectangular container filled with 200 mL of a 100 mM sucrose solution. The pond snails were then observed for 3 minutes after their first rasp. While observing, I kept a marker of the beginning of each rasp. Since sucrose is a 'strong' stimulus, we observe that ΔIRI (IRI = Inter Rasp Interval) was zero during the first minute. From this observation, we used the difference between rasp markers to provide an estimate of each rasp duration. On average, the typical duration of a tri-phasic feeding cycle is about 3 seconds [1]. Contrary to that number, our results give a shorter average of rasp duration (Fig. 3.2).

3.3 Results

Our results indicate that Rotenone protracts the feeding cycle. A direct consequence of this result is a decrease in feeding rate. Using a sample size of nine snails per group, we get a 23.084 percent decrease in rasps per minute during the first minute (Fig. 3.3).

The histogram shows a shift in rasp duration. The control group has more than fifty percent of its rasp duration in the two to three second bins. While the treated group has more than fifty percent in the three to four second bins (Fig. 3.1).

3.4 Experiment to Model

Since the numerical simulation emulates feeding behavior with no inter-rasp interval, we attempted to match the model with experimental results. In our hypothesis, we use the fact that SO reacts to sensory stimulus, like sucrose, to change the frequency of rasps [4]. We targeted SO as a possible neuron that is being affected by damage to dopamine cells in the buccal ganglia. Using that hypothesis, we decided to fix all current parameters at zero, except for the constant current being fed into SO.

The result of this experiment, was a change in constant current to SO. Constant current of 10.5 nA yielded about 21 rasps per minute (Fig. 3.4). This resembled the average number of

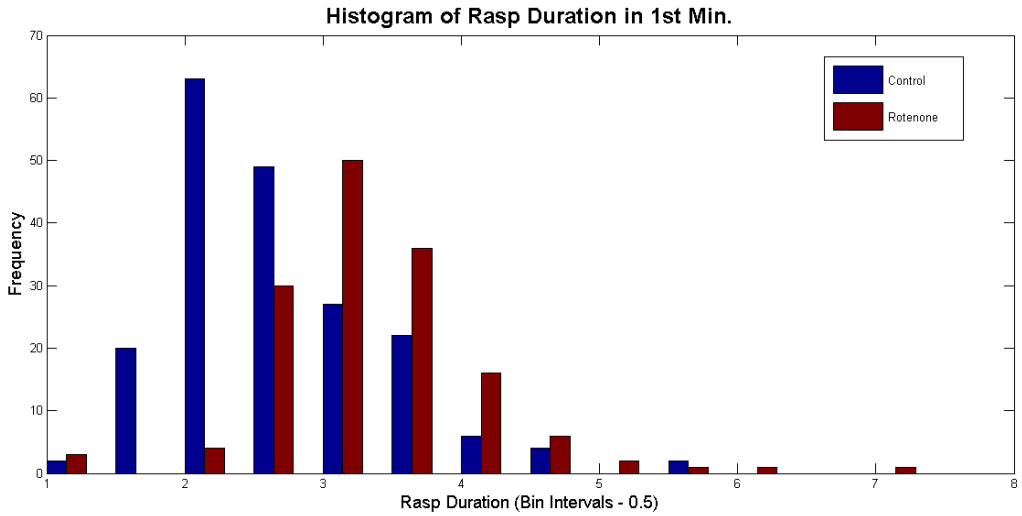

Figure 3.1: Histogram of rasp duration. Blue represents control while red denotes rotenone. In the vertical bar, we are measuring how many times an event occurs in a certain interval. The horizontal axis is time and bin intervals of size 0.5 of a second.

rasps in healthy snails. We then changed the current parameter to 9.2 *nA* to yield about 17 rasps per minute (Fig. 3.5). This resembled the average number of rasps in rotenone treated snails. One important observation is that this choice of parameter is not unique and tuning the model to match experimental data can be done using other parameter choices.

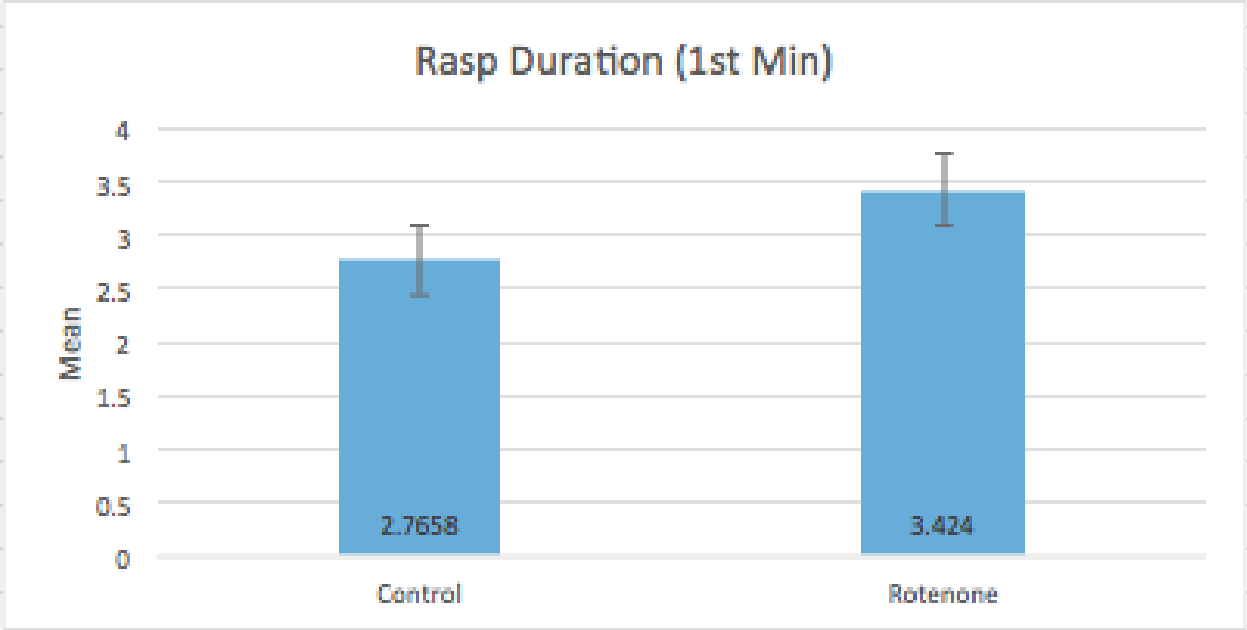

Figure 3.2: Average rasp duration in sucrose. Both the control and treated group had a sample size of nine snails ($n = 9$). The vertical axis is average rasp duration. The results were, Control = 2.7658 *ms* and Rotenone = 3.424 *ms*, with $P < 0.05$.

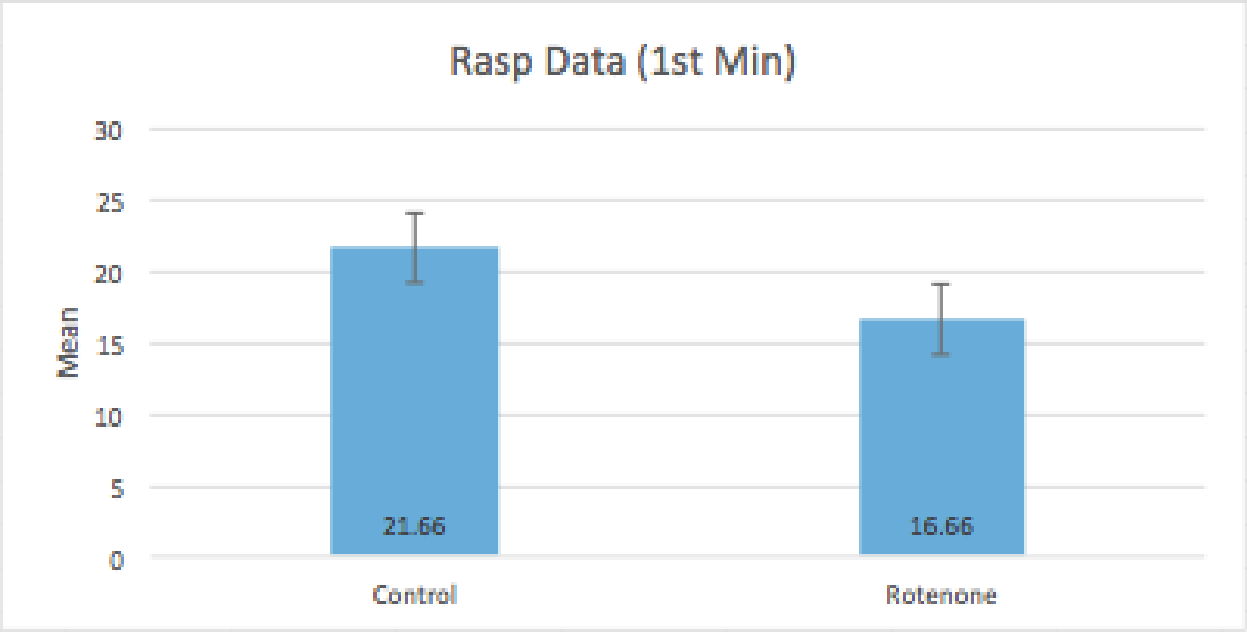

Figure 3.3: Average number of rasps during the first minute. Both the control and treated group had a sample size of nine snails ($n = 9$). This image is directly related to Fig. (3.2). This data was statistically significant, $P < 0.05$.

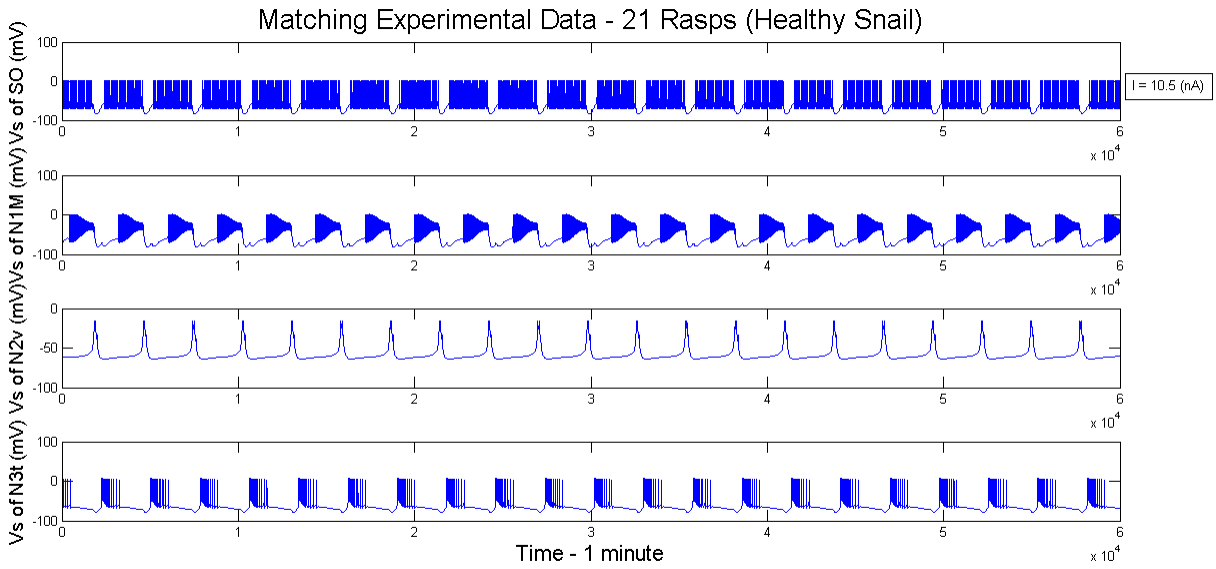

Figure 3.4: We fixed a constant current to SO of 10.5 *nA*, while all other current were fixed at zero. This produced about 21 rasps to match the avgerage number of raps in the healthy group. The vertical axis is voltage measured in millivolts, while the horizontal axis is time measured in milliseconds for a total of one minute.

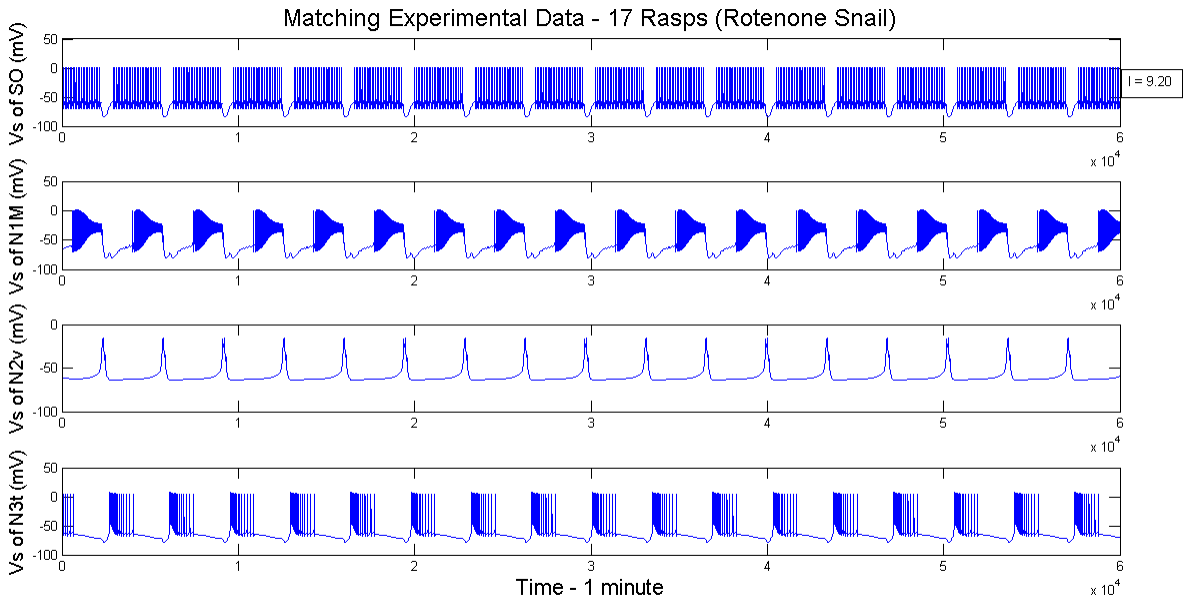

Figure 3.5: We fixed a constant current to SO of 9.2 *nA*, while all other current were fixed at zero. This produced about 17 rasps to match the avgerage number of raps in the rotenone treated group. The vertical axis is voltage measured in millivolts, while the horizontal axis is time measured in milliseconds for a total of one minute.

CHAPTER IV

CONCLUSION

In conclusion, we were able to implement a numerical algorithm to solve the nonlinear system describing feeding in *Lymnaea stagnalis*. The simulation faithfully replicated qualitative features seen in physiological recordings. Furthermore, we investigated some of the basic properties of the system. In particular, the systems sensitivity to current parameters. We showed that with a particular set of currents, the solution of the system enters periodic behavior. In addition, we applied the model to laboratory work on Parkinson's disease. This application allowed us to postulate a possible mechanism of Rotenone's affect on the feeding system.

This project has led to an array of future explorations. For example, we would like to search for dopamine receptors on CPG neurons. This would further justify the fact that dopamine damage leads to a deficit in motor behavior. I will also attempt to record neural activity from Rotenone treated CPG neurons. Mathematically, we would like to explore other properties of the model using tools like Fourier analysis and dynamical systems.

BIBLIOGRAPHY

[1] P. R. BENJAMIN, *Distributed network organization underlying feeding behavior in the mollusk lymnaea*, Neural Systems and Circuits, 2 (2012), pp. 4–4.

[2] A. L. HODGKIN AND A. F. HUXLEY, *A quantitative description of membrane current and its application to conduction and excitation in nerve*, The Journal of Physiology, 117 (1952), p. 500.

[3] E. R. KANDEL, J. H. SCHWARTZ, T. M. JESSELL, ET AL., *Principles of Neural Science*, vol. 4, McGraw-Hill New York, 2000.

[4] D. V. VAVOULIS, V. A. STRAUB, I. KEMENES, G. KEMENES, J. FENG, AND P. R. BENJAMIN, *Dynamic control of a central pattern generator circuit: a computational model of the snail feeding network*, European Journal of Neuroscience, 25 (2007), pp. 2805–2818.

[5] Á. VEHOVSZKY, H. SZABÓ, L. HIRIPI, C. J. ELLIOTT, AND L. HERNÁDI, *Behavioural and neural deficits induced by rotenone in the pond snail lymnaea stagnalis. a possible model for parkinson's disease in an invertebrate*, European Journal of Neuroscience, 25 (2007), pp. 2123–2130.

[6] H. R. WILSON, *Simplified dynamics of human and mammalian neocortical neurons*, Journal of Theoretical Biology, 200 (1999), pp. 375–388.

BIOGRAPHICAL SKETCH

Juan Morales graduated with honors and earned a Bachelors of Science in Mathematics and a minor in Biology from the University of Texas Pan American. During his undergraduate campaign he was a member of student organizations as well as a participant in intramural sports. He has received a Masters of Science in Applied Mathematics from UTPA. As a graduate student he was a recipient of the GAANN Fellowship. He worked as a research associate as well as a teaching assistant for the department.

He attended the 2013 SACNAS National Conference where he presented his research on, "Small Clusters of Neurons: A Mathematical Model". He also attended the 2013 Society for Neuroscience annual meeting and the 2014 Society for Industrial and Applied Mathematicians annual meeting.

He will soon begin doctoral studies in Neurobiology at the University of Texas at San Antonio. He hopes to one day contribute to the growing field of Mathematical Neuroscience.